

Development of High-Speed Fluorescent X-Ray Micro-Computed Tomography

T. Takeda¹, Y. Tsuchiya¹, T. Kuroe², T. Zeniya², J. Wu¹, Thet-Thet-Lwin¹,
T. Yashiro¹, T. Yuasa², K. Hyodo³, K. Matsumura¹, F.A. Dilmanian⁴,
Y. Itai¹, and T. Akatsuka²

¹*Institute of Clinical Medicine, University of Tsukuba, Tsukuba-shi, Ibaraki 305-8575 Japan*

²*Faculty of Engineering, Yamagata University, Yonezawa-shi, Yamagata 992-8510, Japan*

³*Institute of Materials Structure Science, High Energy Acceleration Research Organization, Japan*

⁴*Medical Department, Brookhaven National Laboratory, Upton, NY 11973, USA*

Abstract. A high-speed fluorescent x-ray CT (FXCT) system using monochromatic synchrotron x rays was developed to detect very low concentration of medium-Z elements for biomedical use. The system is equipped with two types of high purity germanium detectors, and fast electronics and software. Preliminary images of a 10mm diameter plastic phantom containing channels filled with iodine solutions of different concentrations showed a minimum detection level of 0.002 mg/ml at an in-plane spatial resolution of 100 μ m. Furthermore, the acquisition time was reduced about 1/2 comparing to previous system. The results indicate that FXCT is a highly sensitive imaging modality capable of detecting very low concentration of iodine, and that the method has potential in biomedical applications.

INTRODUCTION

Fluorescent x-ray technique in non-imaging and planar imaging mode has been used to evaluate very low contents of specific elements in the order of picograms [1]. Using synchrotron x-rays (SR), the method has evolved into fluorescent x-ray computed tomography [2-15], which can reveal cross-sectional distribution of trace elements in the subject. The method was referred to as FXCT only in a later stage when tight collimation of the detector system was used to improve the method's sensitivity [5-15].

Using two kinds of high purity germanium detectors with high detection efficiency, together with front-end electronics and computer interface of high count-rate capability, we constructed a new FXCT system at Tristan accumulation synchrotron storage ring in Tsukuba. The system was used to acquire phantom images at an overall spatial resolution of less than 0.1 mm to acquire the FXCT data shortly. The relatively short data acquisition time was possible not only because of the improved imaging system, but also because of a higher beam intensity resulting from an upgrade of the storage ring, which led to an increase in the maximum ring current from 30 mA to 55 mA. The present preliminary study used the new FXCT system to image a plastic phantom containing channels filled with solutions of different iodine concentrations.

METHODS AND MATERIAL

The experiment was carried out at the bending-magnet beam line AR NE-5A of the Tristan accumulation ring (6.5 GeV) in Tsukuba, Japan. The photon flux in front of the object was approximately 9.3×10^7 photons/mm²/sec for a beam current of 40 mA. The FXCT system consisted of a silicon (111) double crystal monochromator, an x-ray slit, a scanning table for object positioning, two high purity germanium (HPGe) detectors positioned at 90° to the beam, and a transmission x-ray detector. The system's picture and schematic diagram are shown in Fig. 1 and 2, respectively. The white x-ray beam was monochromated to 37 keV x-ray energy. The monochromatic beam was collimated into a 0.1 \times 0.1 mm² pencil beam and used to image the phantom. The two Ge-detectors (LO-AX and IGLET, both from EG-&G ORTEC) and the high-speed electronic system (DSPEC Plus, also EG-&G ORTEC)

were used to collect data at a high count rate. The IGLET Ge detector had a very good energy resolution of 230 eV, compared to the LO-AX detector with 714 eV at resolution, both measured at the iodine $K\alpha$ line of 27.5 keV. The phantom was a 10mm in diameter acrylic cylinder containing three 3.4mm paraxial channels filled with iodine solutions of different concentration. The object was positioned precisely by linear and rotating stages. The two HPGe detectors, were positioned perpendicular to the incident monochromatic x-ray beam at both sides of the phantom and were apertured to a small solid angle to minimize detection of the Compton scattered x-rays while measuring the fluorescent x-rays emitted from the subject. The distances between the detectors and the sample, together with the sizes of the detector and the slits are given in Table 1. At the geometry used, the count rates in the two detectors were almost the same, with the same dead time of about 20%. The CT data collection was carried out by scanning the phantom in the beam at a 0.1mm translational step size, and a 1.2° rotational step size over 180 degrees. The data acquisition time was 5 s for each scanning step.

The transmission detector was a CCD-based-camera, it allowed measurement of the transmitted x-rays simultaneous to the fluorescence x-ray measurement.

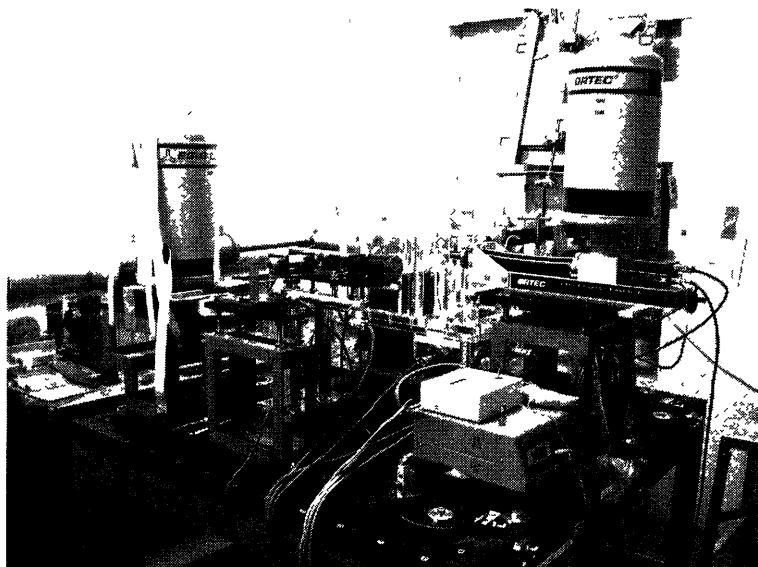


FIGURE 1. Picture of the New FXCT System

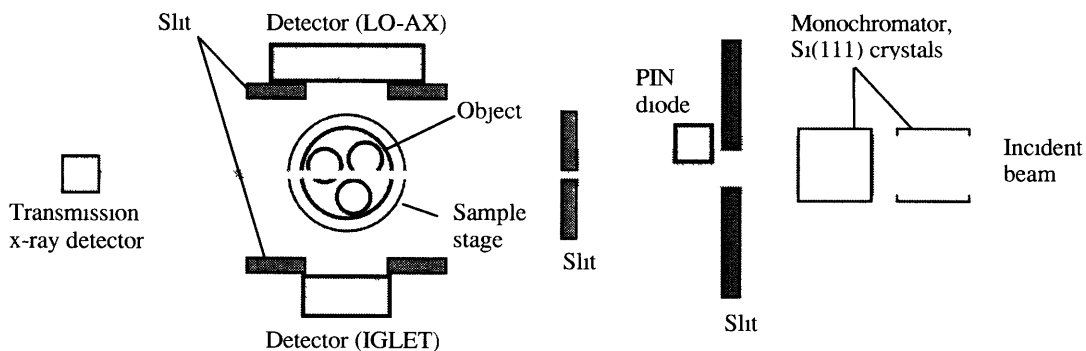


FIGURE 2. Schematic Diagram of the New FXCT System

TABLE 1. Setting Parameters of the X-ray Detectors.

HPGe detector type	Distance of the detector from the Beam	Diameter of the Detector	Detector slit size
LO-AX	100mm	51mm	10mm × 20mm
IGLET	25mm	11mm	open

RESULTS AND DISCUSSIONS

Before constructing the FXCT system, the detectors were characterized using an ^{125}I x-ray source. Figure 3 shows the measured count rate in the two detectors, LO-AX and IGLET, as a function of the incident count rate. The true count rate as a percent of the incident count rate decreased with increasing incident count rate reach in 98% and 90% for LO-AX and IGLET, respectively for a 10,000 incident count/s. Despite this lower count-rate capability, and its slightly lower detection efficiency (because of its smaller thickness), the IGLET detector was valuable because of its has superior energy resolution.

Typical spectra measured from the phantom by LO-AX and IGLET at a 37-keV incident beam energy are shown in Fig 4. The spectra reveal that the finer energy resolution of IGLET compared to LO-AX. The fluorescence $K\alpha$ line of iodine was isolated and fit with background subtraction for spectra at each of all scanning step, and the net counts were calculated. These counts were then used to reconstruct the CT images

Figure 5 shows the FXCT image of the phantom filled with three concentrations of iodine solution, indicating the clear separation of the iodine concentrations at the $0.1 \times 0.1 \text{mm}^2$ spatial resolution and 0.1mm slice thickness. These results indicate a minimum concentration detectability of iodine was 0.002 mg iodine/ml. This fine system performance was achieved at half the data acquisition time if to the previous system because of the improved count rate capability of the system, and a higher beam intensity.

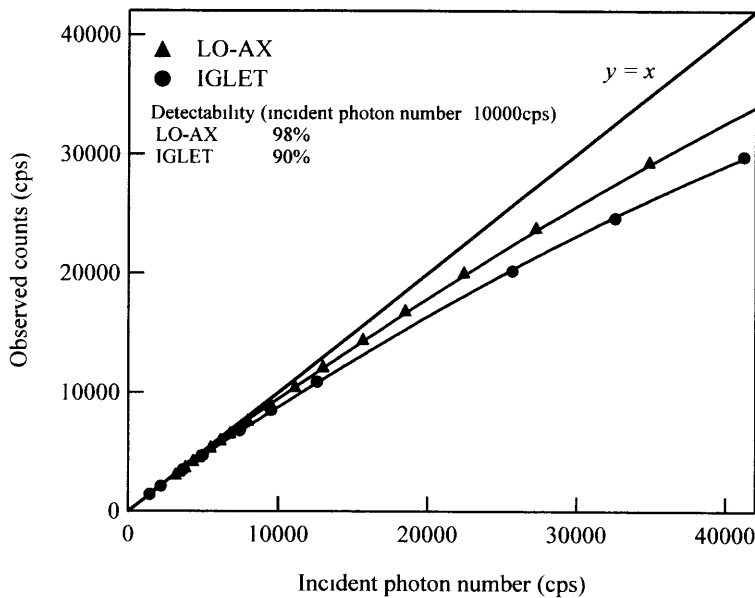


FIGURE 3. Detectability of highly purified Ge detector (LO-AX and IGLET)

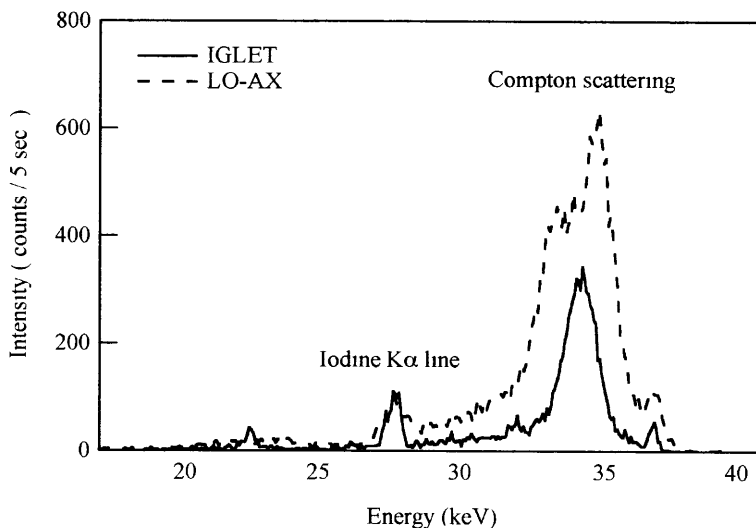


FIGURE 4. Typical Spectra of the Phantom obtained by highly purified Ge detector (LO-AX and IGLET)

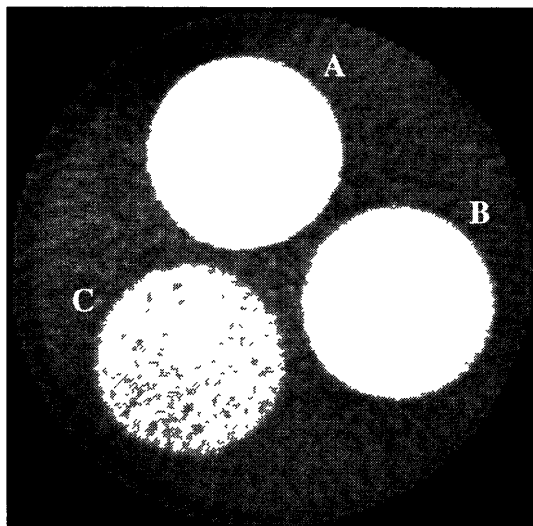


FIGURE 5. FXCT image of a 10 mm in diameter phantom with 3 holes. The 0.005 mg/ml iodine solution are visualized clearly: A) 0.015 mg/ml, B) 0.010 mg/ml, C) 0.005 mg/ml

In conclusion, the new FXCT system equipped with two x-ray detectors and new electronics was constructed and applied successfully. The minimum detected concentration of iodine was 0.002 mg/ml, and the data collection time was smaller compared to the system before the upgrade.

ACKNOWLEDGMENTS

We wish to thank Mr. K. Kobayashi for constructing the FXCT system and preparing the phantom. This research was partially supported by a Grant-in-aid for Scientific Research (#10557084, 01237018 and 13470178) from the Japanese Ministry of Education, Science and Culture, and was carried out under the auspices of the High Energy Accelerator Research Organization (Proposal No. 99G124 and 2001G138).

REFERENCES

- 1 Iida, A., Gohshi, Y., *Handbook on Synchrotron Radiation Vol 4*, edited by S. Ebashi, M. Koch, E. Rubenstein, Elsevier Publisher, Amsterdam 1991, pp 307-348
- 2 Boisseau, P., Grodzins, L., *Hyperfine Interactions* **33**, 283-292 (1987)
- 3 Takeda, T., Maeda, T., Yuasa, T., Akatsuka, T., Itai, Y., *Rev Sci Instrum* **66**, 1471-1473 (1995)
- 4 Takeda, T., Maeda, T., Yuasa, T., Ito, T., Kishi, K., Wu, J., Kazama, M., Hyodo, K., Itai, Y., Akatsuka, T., *Med Imag Tech* **14**, 183-194 (1996)
- 5 Takeda, T., Akiba, M., Yuasa, T., Akatsuka, T., Kazama, M., Hoshino, A., Watanabe, Y., Hyodo, K., Dilmanian, F. A., Akatsuka, T., Itai, Y., *SPIE* **2708**, 685-695 (1996)
- 6 Yuasa, T., Akiba, M., Takeda, T., Kazama, M., Hoshino, Y., Watanabe, Y., Hyodo, K., Dilmanian, F. A., Akatsuka, T., Itai, Y., *IEEE Trans Nucl Sci* **44**, 54-62 (1997)
- 7 Rust, G. F., Weigelt, J., *IEEE Trans Nucl Sci* **45**, 75-88 (1998)
- 8 Takeda, T., Yu, Q., Yashiro, T., Zeniya, T., Yuasa, T., Wu, J., Hasegawa, Y., Thet-Thet-Lwin, Hyodo, K., Dilmanian, F. A., Akatsuka, T., Itai, Y., *Nucl Instrum & Meth* **A467-468**, 1318-1321 (2001)
- 9 Yu, Q., Takeda, T., Yuasa, T., Hasegawa, Y., Wu, J., Thet-Thet-Lwin, Hyodo, K., Dilmanian, F. A., Itai, Y., Akatsuka, T., *J Synchrotron Rad* **8**, 1030-1034 (2001)
- 10 Takeda, T., Zeniya, T., Wu, J., Yu, Q., Thet-Thet-Lwin, Yashiro, T., Itai, Y., Yuasa, T., Akatsuka, T., Dilmanian, F. A., *SPIE* **4503**, 299-309 (2001)
- 11 Takeda, T., Yu, Q., Yuasa, T., Hasegawa, Y., Yashiro, T., Itai, Y., *SPIE* **3772**, 258 (1999)
- 12 Takeda, T., Momose, A., Yu, Q., Wu, J., Hyodo, K., Akatsuka, T., Itai, Y., *Cellular & Molecular Biology* **46**, 1077 (2000)
- 13 Yu, Q., et al., *Med Imag Tech* **18**, 805-816 (2000)
- 14 Simionovic, A., Chukalina, M., Vekemans, B., Lemelle, L., Gillet, Ph., Schroer, Ch., Lengeler, B., Schroder, W., Jeffries, T., *SPIE* **3772**, 304 (1999)
- 15 Takeda, T., Zeniya, T., Wu, J., Thet-Thet-Lwin, Yu, Q., Tsuchiya, Y., Yashiro, T., Yuasa, T., Rao, D. V., Hyodo, K., Dilmanian, F. A., Itai, Y., Akatsuka, T., "Biomedical imaging by fluorescent x-ray micro-computed tomography" in *Joint Symposium on Bio-Sensing and Bio-Imaging 2001*, (2002) pp 112-117